

Edge Caching for Coverage and Capacity-aided Heterogeneous Networks

Ejder Baştug[◊], Mehdi Bennis[†], Marios Kountouris[◊] and Mérouane Debbah^{◊,◦}

[◊]Large Networks and Systems Group (LANEAS), CentraleSupélec,
Université Paris-Saclay, 3 rue Joliot-Curie, 91192 Gif-sur-Yvette, France

[†]Centre for Wireless Communications, University of Oulu, Finland

[◦]Mathematical and Algorithmic Sciences Lab, Huawei France R&D, Paris, France

{ejder.bastug, merouane.debbah}@centralesupelec.fr, marios.kountouris@huawei.com, bennis@ee.oulu.fi

Abstract—A two-tier heterogeneous cellular network (HCN) with intra-tier and inter-tier dependence is studied. The macro cell deployment follows a Poisson point process (PPP) and two different clustered point processes are used to model the cache-enabled small cells. Under this model, we derive approximate expressions in terms of finite integrals for the average delivery rate considering inter-tier and intra-tier dependence. On top of the fact that cache size drastically improves the performance of small cells in terms of average delivery rate, we show that rate splitting of limited-backhaul induces non-linear performance variations, and therefore has to be adjusted for rate fairness among users of different tiers.

Index Terms—edge caching, clustered point processes, heterogeneous cellular networks, stochastic geometry

I. INTRODUCTION

Caching in heterogeneous cellular networks (HCN) significantly improves the system performance, and is of cardinal importance especially in limited-backhaul settings [1], [2]. However, existing stochastic geometry-based analyses of caching in heterogeneous networks [3], [4] ignore the impact of limited-backhaul and consider multiple tiers of mutually independent point processes. To remedy to this situation, this paper analyzes the benefits of edge caching in such wireless deployment conditions.

Consider a heterogeneous network consisting of mobile users, clustered cache-enabled small base stations (SBSs), macro base stations (MBSs) and central routers (CRs) for the backhaul. For SBSs, we shall consider two different topologies: 1) coverage-aided and 2) capacity-aided deployments. Coverage-aided deployment follows a *Poisson hole process* (PHP) while capacity-aided deployment is modeled using a *Matérn cluster process* (MCP). This models inter-tier and intra-tier dependence, respectively. Due to the multi-tier dependence and the non-tractability of the considered point processes, an exact calculation of the interference and key performance metrics seems unfeasible. Hence, we restrict ourselves to approximations in the form of finite integrals and validate their behavior via numerical results.

This hierarchical model exploiting random spanning trees hides the algorithmic details of such a complex network, yet

This research has been supported by the ERC Starting Grant 305123 MORE (Advanced Mathematical Tools for Complex Network Engineering), the project BESTCOM, the Academy of Finland CARMA project and TEKES grant (2364/31/2014).

allows for tractable mathematical expressions to characterize the overall performance of such an heterogeneous network. We show that while the average delivery rate of small cell users (SUs) can be improved by adding more storage per SBS, the backhaul rate splitting among tiers induces non-linear performance variations and requires adjustments for the rate fairness.

II. SYSTEM MODEL

The system model is composed of MBSs, cache-enabled clustered SBSs, CRs and mobile users. We focus on two different topologies as in [5].

A. Coverage-Aided Topology

We model a heterogeneous cellular network which consists of MBSs and cache-enabled SBSs. The MBSs are modeled by an independent homogeneous planar Poisson point process (PPP) of intensity λ_{mc} , denoted by $\Phi_{mc} = \{y_i\}_{i \in \mathbb{N}}$ where y_i denotes the location of the i -th MBS. Additionally, the *potential* SBSs are located according to another independent homogeneous PPP of intensity $\lambda_{sc'}$, denoted by $\Phi_{sc'} = \{x'_i\}_{i \in \mathbb{N}}$ where x'_i represents the location of the i -th SBS. We suppose that each MBS has an exclusion region which is made of a disk with radius R_c centered at the position of MBS. Assuming that the aim of SBSs is to fill the coverage holes of MBSs to provide a better service to users, these SBSs are deployed outside of the exclusion regions of MBSs. Therefore, the deployed SBSs form clusters according to a *Poisson hole process* (Cox process) as follows [6].

Definition 1 (Clustering process of coverage-aided SBSs). *Let Φ_{mc} be a homogeneous PPP of intensity λ_{mc} for MBSs and $\Phi_{sc'}$ be an independent and homogeneous PPP of intensity $\lambda_{sc'}$ for potential SBSs, with $\lambda_{sc'} > \lambda_{mc}$. For each $y \in \Phi_{mc}$, remove all the points in*

$$\Phi_{sc'} \cap \mathcal{B}(y, R_c) \quad (1)$$

where $\mathcal{B}(y, R_c)$ is the ball of radius R_c centered at y . Then, the remaining points of $\Phi_{sc'}$ form clusters, known as the *Poisson hole process* Φ_{sc} and represent the deployed SBSs. Moreover, this process has the intensity of

$$\lambda_{sc} = \lambda_{sc'} \exp(-\lambda_{mc} \pi R_c^2). \quad (2)$$

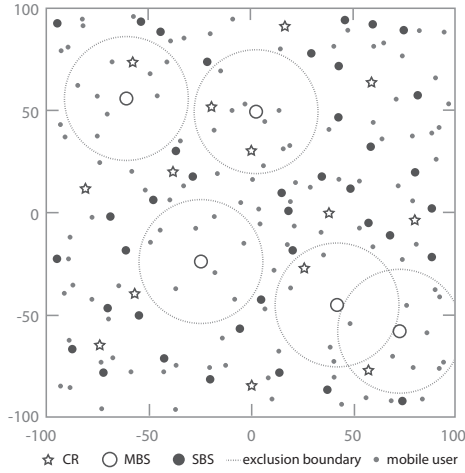


Figure 1: An illustration of the coverage-aided deployment.

On the other hand, CRs are distributed in the plane according to an independent homogeneous PPP of intensity λ_{cr} , denoted by $\Phi_{\text{cr}} = \{u_i\}_{i \in \mathbb{N}}$. These routers are in charge of providing broadband Internet connection to MBSs and SBSs via backhaul links. Mobile user terminals are also positioned in the whole plane according to an independent homogeneous PPP of intensity λ_{ut} , denoted by $\Phi_{\text{ut}} = \{z_i\}_{i \in \mathbb{N}}$, with $\lambda_{\text{ut}} > \lambda_{\text{mc}}$ and $\lambda_{\text{ut}} > \lambda_{\text{sc}}$. The snapshots of these point processes are given in Fig. 1.

B. Capacity-Aided Topology

Suppose a two-tier heterogeneous cellular network consisting of MBSs and cache-enabled SBSs. The MBSs are distributed according to an independent homogeneous PPP of intensity λ_{mc} , denoted by $\Phi_{\text{mc}} = \{y_i\}_{i \in \mathbb{N}}$ where y_i denotes the position of the i -th MBS. The SBSs are placed in hot-spots to sustain the demand of highly concentrated users, according to an independent *Matérn cluster process* $\Phi_{\text{sc}} = \{x_i\}_{i \in \mathbb{N}}$ whose parent PPP $\Phi_{\text{sc}'}$ has intensity $\lambda_{\text{sc}'}$. The process is given as follows [6].

Definition 2 (Clustering process of capacity-aided SBSs). *Let $\Phi_{\text{sc}'}$ be a parent process modelled by a homogeneous PPP of intensity $\lambda_{\text{sc}'}$. Then, the clustering process of SBSs is given by*

$$\Phi_{\text{sc}} = \bigcup_{x' \in \Phi_{\text{sc}'}} N^{x'} \quad (3)$$

where $N^{x'}$ is a Poisson number of independent and identically distributed (i.i.d.) points with mean \bar{c} , distributed uniformly in the ball $\mathcal{B}(x', R_c)$. Then, the process Φ_{sc} is called *Matérn cluster process* Φ_{sc} and has intensity of

$$\lambda_{\text{sc}} = \lambda_{\text{sc}'} \bar{c}. \quad (4)$$

For the users, we suppose that mobile users (both macro cell users (MUs) and SUs) are distributed on the two-dimensional Euclidean plane, however SUs are highly concentrated in hot-spot regions served by SBSs. From this motivation, we assume that all mobile users are distributed according to a Cox process $\Phi_{\text{ut}} = \{z_i\}_{i \in \mathbb{N}}$ [6]. In particular, the population centers of

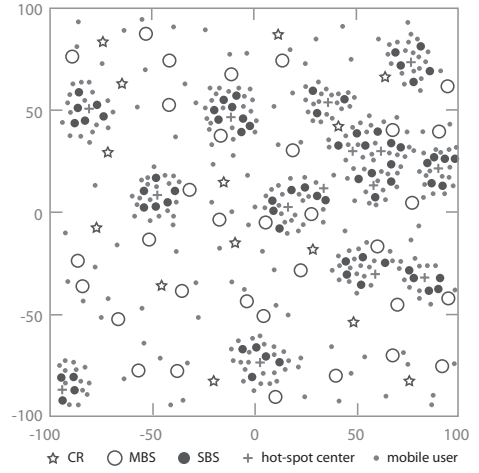


Figure 2: An illustration of the capacity-aided deployment.

radius R_c are drawn from the parent PPP $\Phi_{\text{sc}'}$, where SUs in these clusters are distributed uniformly at random and are covered by SBSs forming a Matérn cluster process Φ_{sc} . By doing so, these mobile users are (on average) covered by their SBSs deployed in these hot-spot areas.

Recalling \bar{c} as the average number of SBSs per cluster, the density of active SUs per cluster is then $\lambda_{\text{ut-s}} = \frac{\bar{c}}{\pi R_c^2}$. The MUs distributed in the rest of the network follow a PPP with density $\lambda_{\text{ut-m}}$ and are served by their own MBSs. For convenience, we consider that each MBS serves only one MU on average and the same holds for each SBS and its user. With this consideration in mind, the densities of MUs and SUs are equal to that of the MBSs and SBSs, respectively. Under this setting, the MUs and SUs form a Cox process with density $\lambda_{\text{ut}} = \lambda_{\text{mc}} + \lambda_{\text{sc}}$, clustered in hot-spots and uniformly distributed elsewhere. On the other hand, we consider that CRs are modeled by an independent homogeneous PPP of intensity λ_{cr} , denoted by $\Phi_{\text{cr}} = \{u_i\}_{i \in \mathbb{N}}$. A snapshot of the topology is depicted in Fig. 2.

C. Signal Model, Connectivity and Backhaul

The downlink transmissions of MBSs and SBSs occur at the same frequency with reuse factor 1. The transmit power is P_{mc} for each MBS and P_{sc} for each SBS. All nodes (MBSs, SBSs and users) have single antenna. Having an MBS positioned at y and receiver at z (or simply call as transmitter y and user z), the channel coefficient is denoted by $h_{y,z} \in \mathbb{C}$. In case of SBS as a transmitter, the channel coefficient between transmitter x and user z is given by $g_{x,z} \in \mathbb{C}$. All the channel power coefficients are i.i.d. exponential random variables (Rayleigh fading) with $\mathbb{E}[|h_{y,z}|^2] = 1$ and $\mathbb{E}[|g_{x,z}|^2] = 1$. Supposing that the downlink rate of the typical user is a function of received signal-to-interference ratio (SIR), the target rate of signaling MBS and SBS are given by τ_{mc} and τ_{sc} respectively.

Each user is either associated to the nearest MBS or nearest SBS. The backhaul connection of each base station is provided from its nearest CR. Supposing that each CR has a sufficiently high-capacity broadband Internet connection,

MBSs and SBSs are connected to their nearest CRs via error-free *wired* backhaul links. In particular, each CR has a total capacity of C_{cr} , which is an exponentially distributed random variable with mean μ .

D. Caching

We assume that the global content popularity distribution of users follow a power law defined as [7]

$$f_{\text{pop}}(f, \eta) = \begin{cases} (\eta - 1) f^{-\eta}, & f \geq 1, \\ 0, & f < 1, \end{cases} \quad (5)$$

where f indicates a point in the support of the corresponding content and the parameter η models the steepness of the distribution. In this work, we assume that f_{pop} is perfectly known at the SBSs. In $f_{\text{pop}}(f, \eta)$, the contents in the interval $[1, F)$ are *cacheable* and called as *catalogue*, whereas the remaining part $[F, \infty]$ is called as non-cacheable contents (i.e., voice traffic, online gaming and sensor information). An interval $[f, f + \Delta f)$ in the support of $f_{\text{pop}}(f, \eta)$ is considered as the probability of f -th content. Indeed, we assume that each content in the catalogue has a fixed length and called as *chunk*. Each chunk can belong to a part of cacheable video file, audio or picture and so on. In fact, storing/distributing fixed-length chunks is one of the key principle in content centric networks [8]. Therefore, even though we use the term "content" in the paper, the function $f_{\text{pop}}(f, \eta)$ is actually a chunk popularity distribution. Each SBS has a storage capacity of F_{sc} contents/chunks, with $1 \leq F_{\text{sc}} \leq F$.

E. Hierarchical Model

The coverage and capacity-aided deployments of SBSs together with MBSs, users and CRs can be modeled as random stationary graphs (hierarchical spanning trees) [9]. In particular, a random hierarchical tree whose root node is a CR located at u is given by $\Psi = \{(u, \mathbf{v}_u)\}$, where \mathbf{v}_u is a mark vector containing all random variables associated with the CR. In particular, the mark vector \mathbf{v}_u contains information of MBSs and SBSs (with their users) which are associated to the CR at u , such as:

- N_{mc} : The number of MBSs connected to the CR located at u . The vector $\mathbf{r}_{\text{mc}} \in \mathbb{C}^{1 \times N_{\text{mc}}}$ is the relative position vector of those MBSs connected to the CR at u . Therein, each element $r_{u,y}$ represents the distance from CR at u to MBS at y . These positions are conditioned on N_{mc} .
- N_{mu} : The number of users connected to an MBS located at $y \in \{\mathbf{r}_{\text{mc}}\}$. The vector $\mathbf{r}_{\text{mu}} \in \mathbb{C}^{1 \times N_{\text{mu}}}$ is the relative positions of those MUs which are conditioned on N_{mu} . Each element $r_{y,z}$ represents distance from MBS at y to its user z .
- N_{sc} : The number of SBSs connected to the CR located at u . The vector $\mathbf{r}_{\text{sc}} \in \mathbb{C}^{1 \times N_{\text{sc}}}$ is the relative positions of those SBSs connected to the CR at u . Here, each element $r_{u,x}$ represents the distance from CR at u to SBS at x . These positions are conditioned on N_{sc} .
- N_{su} : The number of users connected to an SBS located at $x \in \{\mathbf{r}_{\text{sc}}\}$. The vector $\mathbf{r}_{\text{su}} \in \mathbb{C}^{1 \times N_{\text{su}}}$ is the relative

positions of users connected to the SBS at $x \in \{\mathbf{r}_{\text{sc}}\}$. They are conditioned on N_{su} . Each element $r_{x,z}$ represents distance from SBS at x to its user at z .

III. PERFORMANCE METRICS

For the performance metrics of coverage and capacity-aided deployments, we first start by defining SIR.

Definition 3. *The SIR of a typical user connected to an MBS (namely typical MU) located at random position y is defined as*

$$\text{SIR}_{\text{mu}} \triangleq \frac{P_{\text{mc}} h_y \ell(y)}{I_{\text{mm}} + I_{\text{sm}}} \quad (6)$$

where $\ell(y) = \|y\|^{-\alpha}$ is the standard power-law path loss function (unless otherwise stated) with exponent α , $I_{\text{mm}} = \sum_{y_i \in \Phi_{\text{mc}} \setminus \{y\}} P_{\text{mc}} h_{y_i} \ell(y_i)$ is the cumulative interference from other MBSs except the serving cell at y , and $I_{\text{sm}} = \sum_{x_i \in \Phi_{\text{sc}}} P_{\text{sc}} g_{x_i} \ell(x_i)$ is the total interference from clustered SBSs. Similarly, the SIR of a typical user connected to an SBS (namely typical SU) located at random position x is given by

$$\text{SIR}_{\text{su}} \triangleq \frac{P_{\text{mc}} g_x \ell(x)}{I_{\text{ss}} + I_{\text{sm}}} \quad (7)$$

where $I_{\text{ss}} = \sum_{x_i \in \Phi_{\text{sc}} \setminus \{x\}} P_{\text{sc}} g_{x_i} \ell(x_i)$ is the cumulative interference from other clustered SBSs except the serving cell at x , and $I_{\text{sm}} = \sum_{y_i \in \Phi_{\text{mc}}} P_{\text{mc}} h_{y_i} \ell(y)$ is the total interference from MBSs.

The amount of backhaul rate allocated to typical users are defined by the following policy.

Definition 4 (Backhaul Rate Splitting Policy). *Following the hierarchical model, suppose that a typical user located at $z \in \{\mathbf{r}_{\text{mu}}\}$ (typical MU) is connected to the MBS at $y \in \{\mathbf{r}_{\text{mc}}\}$, and this MBS is connected to the nearest CR at u . Then, the rate of backhaul link to the MBS at y is given as*

$$R'_{\text{mu}} \triangleq \frac{\gamma C_{\text{cr}}}{\mathbb{E}[N_{\text{mc}} N_{\text{mu}}]}, \quad (8)$$

where $\gamma \in [0, 1]$ is a fraction of capacity allocated to the MBSs. In case of SBS, in a similar vein, a typical user located at $z \in \{\mathbf{r}_{\text{su}}\}$ is connected to the SBS at $x \in \{\mathbf{r}_{\text{sc}}\}$ whose CR is at u . Then, the rate of backhaul link to the SBS is given as

$$R'_{\text{su}} \triangleq \frac{(1 - \gamma) C_{\text{cr}}}{\mathbb{E}[N_{\text{sc}} N_{\text{su}}]}. \quad (9)$$

The expectation above is taken over the topology generated by the point processes of users and base stations. We now define our main performance metric as follows.

Definition 5 (Delivery Rate). *The delivery rate of a typical user connected to an MBS is defined as*

$$R_{\text{mu}} \triangleq \begin{cases} \tau_{\text{mc}}, & \text{if } \log(1 + \text{SIR}_{\text{mu}}) > \tau_{\text{mc}} \text{ and } R'_{\text{mu}} > \tau_{\text{mc}}, \\ 0, & \text{otherwise.} \end{cases} \quad (10)$$

Similarly, the delivery rate of a typical user connected to an SBS is defined as

$$R_{\text{su}} \triangleq \begin{cases} \tau_{\text{sc}}, & \text{if } \log(1 + \text{SIR}_{\text{su}}) > \tau_{\text{sc}} \text{ and } R'_{\text{su}} > \tau_{\text{sc}}, \\ \tau_{\text{sc}}, & \text{if } \log(1 + \text{SIR}_{\text{su}}) > \tau_{\text{sc}} \text{ and } f_z \in \Delta_x, \\ 0, & \text{otherwise,} \end{cases} \quad (11)$$

where f_z represents the content requested by the typical SU and Δ_x is the cache of the SBS.

We are now ready to give the expressions for the average delivery rate of typical MUs and SUs.

IV. MAIN RESULTS

Theorem 1 (Average Delivery Rate of Typical MU). *The average delivery rate of a typical user connected to the nearest MBS cell in coverage-aided deployment is approximated as*

$$\bar{R}_{\text{mu}}^{(\text{cov})} \approx \tau_{\text{mc}} B_1^{(\text{cov})} B_2^{(\text{cov})} \quad (12)$$

where $B_1^{(\text{cov})}$ and $B_2^{(\text{cov})}$ are given in (14) and (18) respectively. Therein, Laplace transforms and other related function definitions are given below $B_1^{(\text{cov})}$, and $F(x, y; z; w)$ is the hypergeometric function. For capacity-aided deployment, we have

$$\bar{R}_{\text{mu}}^{(\text{cap})} \approx \tau_{\text{mc}} B_1^{(\text{cap})} B_2^{(\text{cap})} \quad (13)$$

where $B_1^{(\text{cap})}$ and $B_2^{(\text{cap})}$ are given in (19) and (24) respectively.

Proof: See Appendix C.1 in [10]. \blacksquare

Remark 1. *These expressions are cumbersome but numerically easy to compute. The terms B_1 and B_2 capture the downlink and backhaul behaviour respectively.*

$$B_1^{(\text{cov})} = \int_0^{R_c} e^{-\frac{(e^{\tau_{\text{mc}}}-1)}{P_{\text{mc}} r_{\text{mc}}^{-\alpha}}} \mathcal{L}_{I_{\text{mm}}} \left(\frac{e^{\tau_{\text{mc}}}-1}{P_{\text{mc}} r_{\text{mc}}^{-\alpha}} \right) \times \mathcal{L}_{I_{\text{sm}}} \left(\frac{e^{\tau_{\text{mc}}}-1}{P_{\text{mc}} r_{\text{mc}}^{-\alpha}} \right) \frac{k}{\nu} \left(\frac{r_{\text{mc}}}{\nu} \right)^{k-1} e^{-(r_{\text{mc}}/\nu)^k} dr_{\text{mc}} \quad (14)$$

$$\mathcal{L}_{I_{\text{mm}}}(s) = \exp \left(\frac{-s\pi\lambda_{\text{mc}}P_{\text{mc}}(2/\alpha)}{1-2/\alpha} r_{\text{mc}}^{2-\alpha} \times F(1, 1-2/\alpha; 2-2/\alpha; -sP_{\text{mc}}r_{\text{mc}}^{-\alpha}) \right) \quad (15)$$

$$\mathcal{L}_{I_{\text{sm}}}(s) = \exp \left\{ -\lambda_{\text{sc}}' \left(\frac{(sP_{\text{sc}})^{2/\alpha} \pi^2 (2/\alpha)}{\sin(\pi \frac{2}{\alpha})} - \pi R_c^2 A_{\text{mc}}(s, R_c) \right) \right\} \quad (16)$$

$$A_{\text{mc}}(s, R_c) = \frac{1}{\pi R_c^2} \int_0^{2\pi} \int_0^{\sqrt{R_c^2 - r_{\text{mc}}^2 \sin^2 \varphi}} \frac{r dr d\varphi}{1 + s^{-1} P_{\text{sc}}^{-1} r^\alpha} \quad (17)$$

$$B_2^{(\text{cov})} = 1 - \exp \left(-\frac{\tau_{\text{mc}} \lambda_{\text{cr}} (\lambda_{\text{mc}} + \lambda_{\text{sc}}' \exp(-\lambda_{\text{mc}} \pi R_c^2))}{\mu \gamma \lambda_{\text{mc}}^2 \lambda_{\text{ut}}} \right) \quad (18)$$

$$B_1^{(\text{cap})} = \int_0^{R_c} e^{-\frac{(e^{\tau_{\text{mc}}}-1)}{P_{\text{mc}} r_{\text{mc}}^{-\alpha}}} \mathcal{L}_{I_{\text{mm}}} \left(\frac{e^{\tau_{\text{mc}}}-1}{P_{\text{mc}} r_{\text{mc}}^{-\alpha}} \right) \times \mathcal{L}_{I_{\text{sm}}} \left(\frac{e^{\tau_{\text{mc}}}-1}{P_{\text{mc}} r_{\text{mc}}^{-\alpha}} \right) \frac{k}{\nu} \left(\frac{r_{\text{mc}}}{\nu} \right)^{k-1} e^{-(r_{\text{mc}}/\nu)^k} dr_{\text{mc}} \quad (19)$$

$$\mathcal{L}_{I_{\text{mm}}}(s) = \exp \left(\frac{-s\pi\lambda_{\text{mc}}P_{\text{mc}}(2/\alpha)}{1-2/\alpha} r_{\text{mc}}^{2-\alpha} \times F(1, 1-2/\alpha; 2-2/\alpha; -sP_{\text{mc}}r_{\text{mc}}^{-\alpha}) \right) \quad (20)$$

$$\mathcal{L}_{I_{\text{sm}}}(s) = \exp \left(-\lambda_{\text{sc}}' \int_{\mathbb{R}^2} \left(1 - \exp(-\bar{c}\nu(s, y)) \right) dy \right) \quad (21)$$

$$\nu(s, y) = \int_{\mathbb{R}^2} \frac{f(x)}{1 + (sP_{\text{sc}}\ell(x-y))^{-1}} dx \quad (22)$$

$$f(x) = \begin{cases} \frac{1}{\pi R_c^2}, & \text{if } \|x\| < R_c, \\ 0, & \text{otherwise.} \end{cases} \quad (23)$$

$$B_2^{(\text{cap})} = 1 - \exp \left(-\frac{\tau_{\text{mc}} \lambda_{\text{cr}}}{\mu \gamma \lambda_{\text{ut}} - m} \right) \quad (24)$$

Theorem 2 (Average Delivery Rate of Typical SU). *The average delivery rate of the typical user connected to the nearest SBS in coverage-aided deployment is approximated as*

$$\bar{R}_{\text{su}}^{(\text{cov})} \approx \tau_{\text{sc}} C_1^{(\text{cov})} C_2^{(\text{cov})} + \tau_{\text{sc}} C_1^{(\text{cov})} C_3^{(\text{cov})} \quad (25)$$

$$-\tau_{\text{sc}} C_1^{(\text{cov})} C_2^{(\text{cov})} C_3^{(\text{cov})} \quad (26)$$

where $C_1^{(\text{cov})}$, $C_2^{(\text{cov})}$ and $C_3^{(\text{cov})}$ are given in (29), (33) and (34) respectively. Therein, Laplace transforms and other related function definitions are given below $C_1^{(\text{cov})}$. For capacity-aided deployment, we have

$$\bar{R}_{\text{su}}^{(\text{cap})} \approx \tau_{\text{sc}} C_1^{(\text{cap})} C_2^{(\text{cap})} + \tau_{\text{sc}} C_1^{(\text{cap})} C_3^{(\text{cap})} \quad (27)$$

$$-\tau_{\text{sc}} C_1^{(\text{cap})} C_2^{(\text{cap})} C_3^{(\text{cap})} \quad (28)$$

where $C_1^{(\text{cap})}$, $C_2^{(\text{cap})}$ and $C_3^{(\text{cap})}$ are given in (35), (39) and (40) respectively.

Proof: See Appendix C.2 in [10]. \blacksquare

Remark 2. *The terms C_1 , C_2 and C_3 incorporate the downlink, backhaul and caching aspects respectively.*

$$C_1^{(\text{cov})} = \int_0^{R_c} e^{-\frac{(e^{\tau_{\text{sc}}}-1)}{P_{\text{sc}} r_{\text{sc}}^{-\alpha}}} \mathcal{L}_{I_{\text{ss}}} \left(\frac{e^{\tau_{\text{sc}}}-1}{P_{\text{sc}} r_{\text{sc}}^{-\alpha}} \right) \times \mathcal{L}_{I_{\text{ms}}} \left(\frac{e^{\tau_{\text{sc}}}-1}{P_{\text{sc}} r_{\text{sc}}^{-\alpha}} \right) \frac{k}{\nu} \left(\frac{r_{\text{sc}}}{\nu} \right)^{k-1} e^{-(r_{\text{sc}}/\nu)^k} dr_{\text{sc}} \quad (29)$$

$$\mathcal{L}_{I_{\text{ss}}}(s) = \exp \left(\frac{-s\pi\lambda_{\text{sc}}'P_{\text{sc}}(2/\alpha)}{1-2/\alpha} r_{\text{sc}}^{2-\alpha} \times F(1, 1-2/\alpha; 2-2/\alpha; -sP_{\text{sc}}r_{\text{sc}}^{-\alpha}) \right) \quad (30)$$

$$\mathcal{L}_{I_{\text{ms}}}(s) = \exp \left\{ -\lambda_{\text{mc}} \left(\frac{(sP_{\text{mc}})^{2/\alpha} \pi^2 (2/\alpha)}{\sin(\pi \frac{2}{\alpha})} - \pi R_c^2 A_{\text{sc}}(s, R_c) \right) \right\} \quad (31)$$

$$A_{sc}(s, R_c) = \frac{1}{\pi R_c^2} \int_0^{2\pi} \int_0^{r_{sc} \cos \varphi + \sqrt{R_c^2 - r_{sc}^2 \sin^2 \varphi}} \frac{r dr d\varphi}{1 + s^{-1} P_{mc}^{-1} r^\alpha} \quad (32)$$

$$C_2^{(cov)} = 1 - \exp\left(-\frac{\tau_{sc} \lambda_{cr} (\lambda_{mr} + \lambda_{sc})}{\mu \gamma \lambda_{sc}^2 \lambda_{ut}}\right) \quad (33)$$

$$C_3^{(cov)} = 1 - (1 + F_{sc})^{-\eta} \quad (34)$$

$$C_1^{(cap)} = \int_0^{R_c} e^{-\frac{(e^{\tau_{sc}} - 1)}{P_{sc} r_{sc}^{-\alpha}}} \mathcal{L}_{I_{ss}}\left(\frac{e^{\tau_{sc}} - 1}{P_{sc} r_{sc}^{-\alpha}}\right) \times \mathcal{L}_{I_{ms}}\left(\frac{e^{\tau_{sc}} - 1}{P_{sc} r_{sc}^{-\alpha}}\right) \frac{k}{\nu} \left(\frac{r_{sc}}{\nu}\right)^{k-1} e^{-(r_{sc}/\nu)^k} dr_{sc} \quad (35)$$

$$\mathcal{L}_{I_{ss}}(s) = \exp\left(-\lambda_{sc}' \int_{\mathbb{R}^2} (1 - \exp(-\bar{c}\nu(s, x))) dx\right) \int_{\mathbb{R}^2} (\exp(-\bar{c}\nu(s, x))) f(x) dx \quad (36)$$

$$\nu(s, x) = \int_{\mathbb{R}^2} \frac{f(y)}{1 + (s P_{sc} \bar{\ell}(y-x))^{-1}} dy \quad (37)$$

$$\mathcal{L}_{I_{ms}}(s) = \exp\left(-\lambda_{mc} \frac{(s P_{mc})^{2/\alpha} \pi^2 (2/\alpha)}{\sin(\pi \frac{2}{\alpha})}\right) \quad (38)$$

$$C_2^{(cap)} = 1 - \exp\left(-\frac{\tau_{mc} \lambda_{cr}}{\mu \gamma \lambda_{ut-s}}\right) \quad (39)$$

$$C_3^{(cap)} = 1 - (1 + F_{sc})^{-\eta} \quad (40)$$

V. NUMERICAL RESULTS AND DISCUSSION

In this section, we validate our expressions via Monte-Carlo simulations. First, the impact of backhaul rate splitting ratio γ on the average delivery rate is given in Figs. (3a) and (4a) for coverage and capacity-aided deployments respectively. Indeed, as seen from the figures, a dramatical increase in average delivery rate occurs which confirms our intuitions. The rate of decrement for the typical SU is relatively slow compared to the typical MU. In order to find a balance between average delivery rate of typical MUs and SUs, ensuring rate fairness, the plots show that one has to set γ carefully. In all of these cases, we observe that having caching capabilities at SBSs improves system performance in terms of average delivery rate. In other words, a heterogeneous network consists of MBSs and cache-enabled SBSs allows higher average delivery rates while ensuring fairness between users at different tiers.

Second, the impact of storage size F_{sc} on the average delivery rate is given in Figs. (3b) and (4b) for coverage and capacity-aided deployments respectively. It is shown that increasing storage size of SBSs both in coverage and capacity-aided deployments yields higher average delivery rates. The increment of storage size in coverage-aided deployment is more visible compared to capacity-aided deployment and allows typical SUs to achieve higher rates than typical MUs. Given the fact that caching monotonically improves the overall system performance of SUs, more storage does not seem necessary if one considers a linear cost for storage size, even though more storage is desirable for improving the average delivery rate.

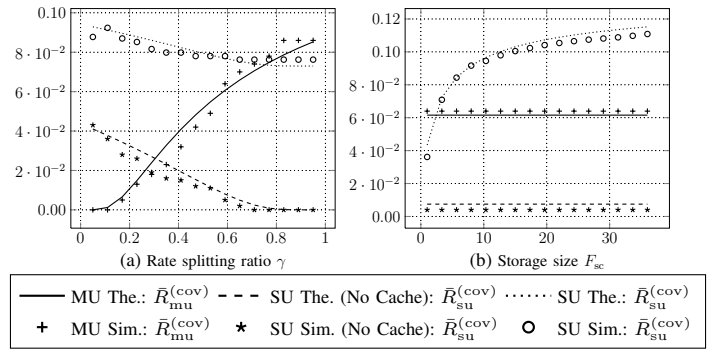


Figure 3: Evolution of average delivery rate in coverage-aided deployment. $\lambda_{cr} = 1.0 \times 10^{-5}$, $\lambda_{mc} = 1.5 \times 10^{-5}$, $\lambda_{sc}' = 5.5 \times 10^{-5}$, $\lambda_{ut-m} = 12.8 \times 10^{-5}$ unit/m²; $P_{mc} = 16$, $P_{sc} = 3$ Watt; $\tau_{mc} = \tau_{sc} = 4$ bits/s/Hz; $\alpha = 4$; $R_c = 80$ meters; $\mu = 30$ bits/s/Hz; $\gamma = 0.6$; $f_0 = 500$ GByte; $F_{sc} = 4$ GByte; $\eta = 1.45$.

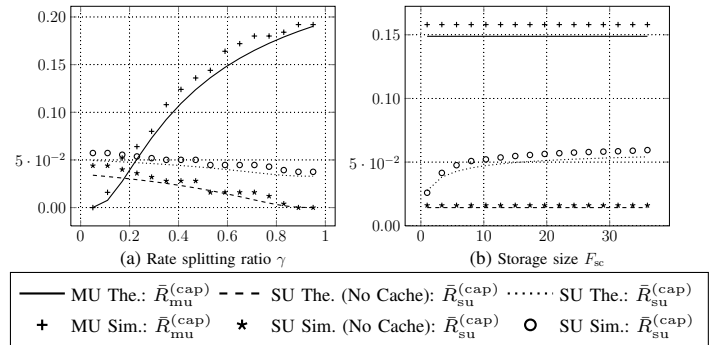


Figure 4: Evolution of average delivery rate in capacity-aided deployment. $\lambda_{cr} = 1.0 \times 10^{-5}$, $\lambda_{mc} = 1.5 \times 10^{-5}$, $\lambda_{sc}' = 1.5 \times 10^{-5}$, $\lambda_{ut-m} = 3.0 \times 10^{-5}$ unit/m²; $\hat{c} = 3$ units; $P_{mc} = 16$, $P_{sc} = 3$ Watt; $\tau_{mc} = \tau_{sc} = 4$ bits/s/Hz; $\alpha = 4$; $R_c = 80$ meters; $\mu = 30$ bits/s/Hz; $\gamma = 0.6$; $f_0 = 500$, $F_{sc} = 4$ GByte; $\eta = 1.45$.

REFERENCES

- [1] E. Baştuğ, M. Bennis, M. Kountouris, and M. Debbah, "Cache-enabled small cell networks: Modeling and tradeoffs," *arXiv preprint arXiv:1405.3477*, 2015.
- [2] K. Shanmugam, N. Golrezaei, A. Dimakis, A. Molisch, and G. Caire, "Femtocaching: Wireless content delivery through distributed caching helpers," *IEEE Transactions on Information Theory*, vol. 59, no. 12, pp. 8402–8413, Dec 2013.
- [3] C. Yang, Y. Yao, Z. Chen, and B. Xia, "Analysis on cache-enabled wireless heterogeneous networks," *IEEE Transactions on Wireless Communications*, vol. 15, no. 1, pp. 131–145, Jan 2016.
- [4] Z. Chen, J. Lee, T. Q. Quek, and M. Kountouris, "Cooperative caching and transmission design in cluster-centric small cell networks," *arXiv preprint arXiv:1601.00321*, 2016.
- [5] N. Deng, W. Zhou, and M. Haenggi, "Heterogeneous cellular network models with dependence," *IEEE Journal on Selected Areas in Communications*, vol. 33, no. 10, pp. 2167–2181, Oct 2015.
- [6] M. Haenggi, *Stochastic geometry for wireless networks*. Cambridge University Press, 2012.
- [7] M. E. Newman, "Power laws, Pareto distributions and Zipf's law," *Contemporary physics*, vol. 46, no. 5, pp. 323–351, 2005.
- [8] V. Jacobson, D. K. Smetters, J. D. Thornton, M. F. Plass, N. H. Briggs, and R. L. Braynard, "Networking named content," in *ACM CoNEXT*. New York, NY, USA: ACM, 2009, pp. 1–12.
- [9] V. Suryaprakash and G. P. Fettweis, "Modeling backhaul deployment costs in heterogeneous radio access networks using spatial point processes," in *proc. of WiOpt 2014*. IEEE, May 2014, pp. 725–732.
- [10] E. Baştuğ, "Distributed caching methods in small cell networks," Ph.D. dissertation, CentraleSupélec, Paris-Saclay University, December 2015. [Online]. Available: <http://goo.gl/C22j1s>